# Numerical simulation of an intervalley transition by the Wigner-function approach

**Lucio Demeio**
Dipartimento di Scienze Matematiche
Università Politecnica delle Marche
Via Brecce Bianche 1, I-60131 Ancona, Italy
**Paolo Bordone** and **Carlo Jacoboni**
INFM - National Research Center on
nanoStructures and bioSystems at Surfaces ($S^3$) and
Dipartimento di Fisica
Università di Modena e Reggio Emilia
Via Campi 213/A, I-41100 Modena, Italy

September 22, 2003

**Abstract**

In this work we present a recently developed transport model, based on the Wigner-function approach and allowing for non-parabolic band profiles. Two scattering mechanisms are included by means of a Boltzmann-like collision operator, describing the collisions between electrons and polar optical and intervalley phonons. The transport equation for the Wigner function is solved by the Splitting-Scheme algorithm. We have chosen a 1-dimensional model band profile, which exhibits satellite valleys, besides the minimum at the center of the Brillouin zone, similar to the band profile of GaAs.

Key-words: Wigner function, Semiconductors, Quantum Transport, Non-parabolic Electron Transport.

# 1 Introduction

The Wigner-function formalism has become a very common tool in the description of the transport properties of semiconductors and electronic devices [1, 2, 3]. All the relevant and realistic applications of this approach, however, have considered until now only those processes which can be adequately described within the single-parabolic-band approximation. Recently, the generalization of the Wigner-function formalism to a multi-band, non-parabolic transport model was introduced [4, 5, 6] for a collisionless system.

In this work, we add a Boltzmann-like collision operator to the transport equations, representing the collisions of electrons with two scattering mechanisms. One is the standard polar optical phonon interaction. A second model scattering mechanism is introduced with phonons with constant energy and deformation potential interaction. Since this scattering allows large momentum transfers, it will be responsible for electron transitions to the band regions of the secondary minima. For analogy with the many valleys model we shell refer to this mechanism as intervalley. The above model will be used to study numerically the transport properties of electrons in a semiconductor.

# 2 The Transport Model

Let $f(x,p,t)$ be the Wigner function of an ensemble of conduction electrons moving in a semiconductor. The single-band evolution equation, in the presence of an arbitrary band profile and under the action of an external potential, is given by [4, 7]

$$\frac{\partial f}{\partial t}(x,p,t) + (Af)(x,p,t) + (\Theta f)(x,p,t) = (Qf)(x,p,t), \tag{1}$$

where the transport operator $A$, describing the action of the periodic potential of the lattice and the pseudodifferential operator $\Theta$, describing the action of the external potential, are defined by

$$(Af)(x,p,t) = \frac{i}{\hbar}\sum_{\mu\in\mathcal{L}} \widehat{\varepsilon}(\mu)\left[f(x+\frac{\mu}{2},p,t) - f(x-\frac{\mu}{2},p,t)\right]e^{ip\mu/\hbar}$$

$$(\Theta f)(x,p,t) = \frac{i}{\hbar}\int \delta V(x,\eta)\widehat{f}(x,\eta,t)e^{-ip\eta/\hbar}\,d\eta.$$

and we have added a collision operator on the right hand side. Here, $\widehat{f}(x,\eta,t)$ is the Fourier transform of the Wigner function with respect to the momentum variable, $\widehat{\varepsilon}(\mu)$, $\mu \in \mathcal{L}$ (being L a vector of the crystal lattice), are the Fourier coefficients of the energy band and $\delta V(x,\eta) = V(x+\eta/2) - V(x-\eta/2)$ is the symbol of the pseudodifferential operator, with $V(x)$ the external potential. We impose the boundary conditions $f(x,p_{max}) = f(x,-p_{max}) = 0$, with $p_{max} = \hbar\pi/a$, and $f(-L,p) = f(L,p) = 0$, that is the we assume that the Wigner function vanishes at the boundary of the simulation region. The choice of the boundary conditions in momentum space, requires that we follow the time evolution of the Wigner function only until all components of the electron population remain well inside the first Brillouin zone. Two scattering mechanisms are included in the collision operator as described in the previous section. For the sake of simplicity, as a first approximation, a 1-dimensional (1-D) Boltzmann-like collision operator is considered. The reduction of the 3-D pronlem to 1-D is obtained by integrating the transport equation along the other two directions, where a thermal distribution and a constant effective mass $m^*$ have been used [1, 8]. The collision operator then results to be:

$$(Qf)(x,p,t) = \int_{-\pi\hbar/a}^{\pi\hbar/a} [\sigma(p',p)f(x,p',t) - \sigma(p,p')f(x,p,t)]\,dp' \tag{2}$$

The scattering cross section $\sigma(p,p')$ is given by the sum of the intervalley and the polar optical cross sections, $\sigma(p,p') = \sigma_{int}(p,p') + \sigma_{opt}(p,p')$, where

$$\sigma_{int}(p,p') = S_{int}\left[(N_0+1)e^{-\bar{\chi}_-^0(p,p')/(k_BT)} + N_0 e^{-\bar{\chi}_+^0(p,p')/(k_BT)}\right] \tag{3}$$

$$\sigma_{opt}(p,p') = S_{opt}\left[(N_1+1)I_-(p,p') + N_1 I_+(p,p')\right] \tag{4}$$

with $S_{int} = m^*D^2/(4\pi\hbar a\rho\hbar\omega_0)$, $S_{opt} = (Q^2/\epsilon_0)(\epsilon_\infty^{-1}-\epsilon_r^{-1})(2\pi m^*/\hbar^2)(\hbar\omega_1/k_BT)/(\hbar a)$ and

$$I_\pm(p,p') = \int_0^\infty e^{-\xi/(k_BT)} \frac{H(\xi+\chi_\pm)}{\sqrt{(k-k')^4 + (2m^*/\hbar^2)^2 + (4m^*/\hbar^2)(k-k')^2(2\xi+\chi_\pm)}}\,d\xi.$$

Here, $H$ is the Heavyside function, $k = p/\hbar$, $\bar{\chi}_\pm^{0,1}(p,p') = \max[-\chi_\pm^{0,1}(k,k'),0]$, $\chi_\pm^{0,1}(k,k') = \varepsilon(k) - \varepsilon(k') \pm \hbar\omega_{0,1}$ and $N_{0,1} = [\exp(-\hbar\omega_{0,1}/(k_BT)-1]^{-1}$ are the phonon occupation numbers. Also, $T = 77$ K is the temperature, $D = 10^9$ eV cm$^{-1}$ the deformation potential, $\rho = 5.33$ g cm$^{-3}$ is the volumic mass, $m^* = 0.067m_e$ is the electron effective mass, $\hbar\omega_0 = 0.0278$ eV and $\hbar\omega_1 = 0.035$ eV are the energies of the intervalley and of the polar optical phonons, respectively, $\epsilon_0$ the vacuum

permittivity, $\epsilon_\infty = 10.67$ and $\epsilon_r = 12.51$ the high frequency and the low frequency permittivities, respectively.

## 3 Numerical results

In this example, we study the time evolution of the Wigner function of an ensemble of electrons under the action of a constant external field and in presence of a non-parabolic band profile. We use the model of Section 2 and solve numerically equation (1) with a modified version of the Splitting-Scheme algorithm [9, 10]. The collision operator is included in the vertical shift together with the pseudodifferential operator that describes the external field. We have chosen a band profile somewhat similar to the band profile of GaAs, with a minimum at $k = 0$ and a second minimum at about half way of the Brillouin zone edge. The band shape, shown in Figure 1, is given by the finite Fourier expansion $\varepsilon(k) = \sum_{\mu \in L} \widehat{\varepsilon}_m(\mu) e^{ik\mu}$, with $\mu = la$ and $\widehat{\varepsilon}(\mu) = b_l e^{i\phi_l}$. Here, $b_0 = 2$ eV, $b_1 = -0.05$ eV, $b_2 = -0.05$ eV and $b_3 = 0.25$ eV, $b_l = 0$, $l > 3$ and $\phi_l = 0$, $l = 0, \ldots$. Also, we take $a = 5.65\ 10^{-8}$ cm (GaAs lattice period), and $L = 5000\ a$ defines the spatial simulation region. An external field $E \approx 21$ kV cm$^{-1}$ acts on a spatial region slightly smaller than the simulation region.

The initial Wigner function corresponds to a statistical mixture and is given by $f(x,p,0) = 1/(\pi\lambda) e^{-(\alpha^2/\lambda^2)(x-x_0)^2 - (p-\hbar k_0)^2/(\alpha\hbar)^2}$, where $x_0$ is the initial average position, $\hbar k_0$ the initial average momentum, $\alpha$ the initial momentum spread and $\lambda/\alpha$ the initial position spread. Also, the normalization $||f|| = \int\int f(x,p) dx\, dp = 1$ has been used. In this example we have $x_0 = -0.1\ L$, $\lambda = L/100$, $k_0 = 0$ and $\alpha = 0.04\ \pi/a$.

We have performed two simulations and compared the results. In one simulation (referred to as R1), only the external field is present (the scattering mechanisms are removed). In a second simulation (R2), we use the full model described in the previous section, including the two scattering mechanisms and the external field. A case similar to (R1) has already been presented in [10].

The results of our simulations are shown in Figures 2 and 3. Figure 2 shows the average momentum (Figure 2A) and the momentum spread (Figure 2B) for the two cases; the solid lines refer to (R2) and the dashed lines to (R1). Finally, Figures 3A and 3B show the Wigner function $f(x,p)$ in phase space at $t = 2$ ps for simulations

(R1) and (R2), respectively. In Figures 3A and 3B, on the floor of the boxes, the graph of the band profile (in the $p$ variable) is also shown for reference.

These results show that, when the collisional mechanisms are not included, the Wigner function tends to remain organized and its shape doesn't change much from the initial Gaussian (see Figure 3A and Figure 2B, which shows that the momentum spread remains constant over this time scale). The second valley at positive $p$ becomes populated, in this case, only by effect of the electric field; the increase in the average momentum is linear at all times, while the average position (not shown here), from about 1 ps onward, suffers a deceleration due to the reversal of the slope of the energy band. In the presence of the collisional mechanisms, both valleys at $p > 0$ and at $p < 0$ become populated (see Figure 3B), due to the effect of the phonon-induced transitions, and the momentum spread grows much larger in time, while the average momentum, after the initial rise, remains almost constant.

**Acknowledgement.** Work partially supported by the U.S. Office of Naval Research (contract No. N00014-98-1-0777) and by the Italian National Research Project COFIN2002 "Mathematical problems of Kinetic Theories".

## References

[1] W. R. Frensley, *Rev. Modern Phys.*, **62**:745-791 (1990).

[2] P. Bordone, M. Pascoli, R. Brunetti, A. Bertoni and C. Jacoboni, Phys. Rev. B **59**(4) (1999) 3060-3069.

[3] C.Jacoboni, R.Brunetti, P. Bordone, and A. Bertoni, Quantum transport ans its simulation with the Wigner-function approach, in *Topics in High Field Transport in Semiconductors*, K. Brennan and P.Paul Ruden, ed. (World Scientific, Singapore 2001), pp.25-61.

[4] L. Demeio, L. Barletti, P. Bordone and C. Jacoboni, Transport Theory and Statistical Physics, **32** (3-4), 321-339 (2003).

[5] L. Demeio, P. Bordone and C. Jacoboni, Proc. XXIII Symposium on Rarefied Gas Dynamics, Whistler, BC, Canada, July 20-25, 2002.

[6] G. Borgioli, G. Frosali and P.F. Zweifel, Proc. XVII International Conference on Transport Theory, London, July 2001, in *Transport Theory Stat. Phys.*, in press.

[7] P. A. Markowich, N. J. Mauser and F. Poupaud, *J. Math. Phys.*, **35**:1066-1094 (1994).

[8] B. Niclot, P. Degond and F. Poupaud, J. Computat. Phys. **78**: 313-349 (1988).

[9] A. Arnold and C. Ringhofer, *SIAM J. of Num. Anal.* **33**: 1622-1643 (1996).

[10] L. Demeio, Proc. 9th Int. Workshop Computat. Electronics, to appear in the *Journal of Computational Electronics*.

# FIGURE CAPTIONS

- Figure 1. Band profile $\varepsilon(k)$ in eV, $-\pi \leq ka \leq \pi$.
- Figure 2. (A) Average momentum $< p > (t)$ and (B) momentum spread $\Delta p(t)$ in units of $\hbar/a$, $0 \leq t \leq 2$ ps. Dashed lines, simulation (R1); solid lines, simulation (R2).
- Figure 3. $f(x, p, t)$ at $t = 2$ ps, $-L \leq x \leq L$, $-\hbar\pi/a \leq p \leq \hbar\pi/a$, for (A) simulation (R1) and (B) simulation (R2). The band profile is shown on the floor for reference.

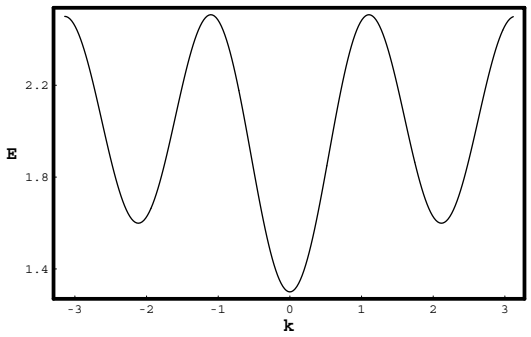


Figure 1: Band profile $\varepsilon(k)$ in eV, $-\pi \leq ka \leq \pi$ .

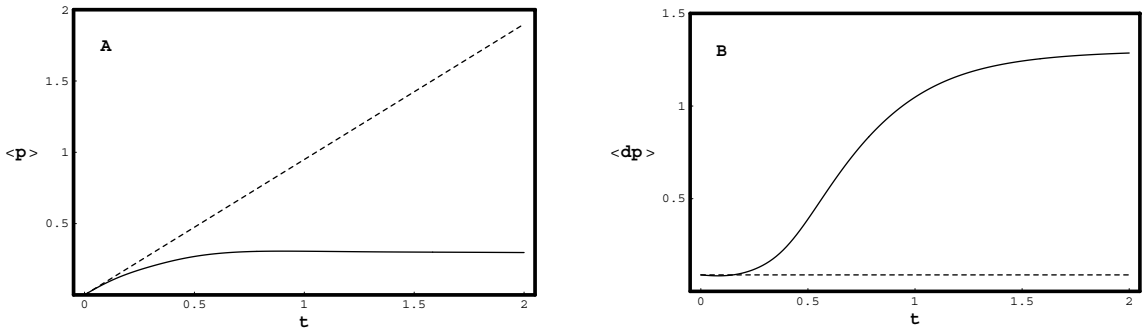


Figure 2: (A) Average momentum $< p > (t)$ and (B) momentum spread $\Delta p(t)$ in units of $\hbar/a$, $0 \leq t \leq 2$ ps. Dashed lines, simulation (R1); solid lines, simulation (R2).

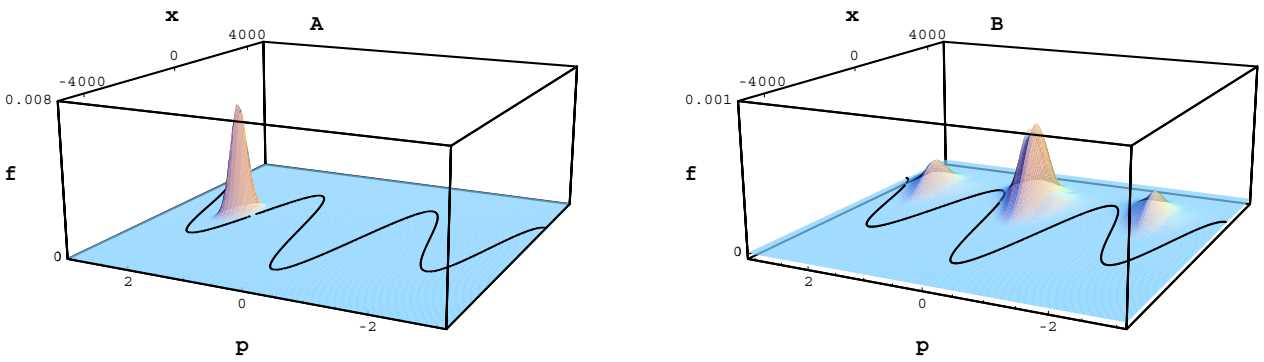


Figure 3: $f(x,p,t)$ at $t = 2$ ps, $-L \leq x \leq L$, $-\hbar\pi/a \leq p \leq \hbar\pi/a$, for (A) simulation (R1) and (B) simulation (R2). The band profile is shown on the floor for reference.